ELSEVIER

Contents lists available at ScienceDirect

Radiotherapy and Oncology

journal homepage: www.thegreenjournal.com



Original Article



Conditioned medium from brachytherapy-irradiated hepatocellular carcinoma cells drives SASP-mediated senescence in naïve cellular counterparts

Josephine Naruhn ^{a,2}, Moritz N. Gröper ^{a,1,2}, Elif Öcal ^a, Lukas Salvermoser ^a, Heidrun Hirner-Eppeneder ^a, Jan N. Schäfer ^a, Philipp M. Kazmierczak ^a, Stephanie Corradini ^b, Justus-Christian Well ^b, Jens Ricke ^a, S. Nahum Goldberg ^c, Matthias Stechele ^a, Marianna Alunni-Fabbroni ^{a,*}

ARTICLE INFO

Keywords: HDR-BT HCC Cellular senescence SASP

ABSTRACT

Background and purpose: Local ablation, including high-dose radiation brachytherapy (HDR-BT), provides a minimally invasive treatment for cancers such as hepatocellular carcinoma (HCC), achieving effective tumor targeting with reduced peri-interventional risk and morbidity. Despite benefits, these treatments face limitations due to tumor recurrence. Cellular senescence might play a key role in therapy resistance by way of tumor cell evasion. This study investigates whether HDR-BT induces cellular senescence *in vitro*, potentially linking these processes to tumor recurrence in HCC.

Material and methods: HCC cell lines (HepG2, Huh7, and Hep3B) were irradiated with 7.5 Gy using an *in vitro* irradiation device. Culture supernatant was collected and transferred to non-irradiated naïve cells. Cell proliferation and senescence were assessed kinetically using BrdU incorporation, Ki-67 immunostaining, and clonogenic assay. Senescence was confirmed by beta-galactosidase staining. Secretome analysis was conducted using a high-throughput proteomic assay.

Results: After irradiation, HCC cells show a transient increase in DNA synthesis, peaking before 72 h without leading to cell division. Exposure of naïve cells to supernatant from irradiated cells replicates these effects, suggesting that the conditioned medium alone can mimic radiation-induced responses. Molecular analysis reveals reduced Ki-67 expression and increased senescence in naïve, incubated cells. Proteomic profiling shows an enrichment of senescence-associated secretory phenotype (SASP) proteins in conditioned medium with exposed naïve cells producing a similar SASP-enriched secretome.

Conclusion: In vitro brachytherapy triggers a bystander effect in HCC cells via SASP-associated proteins inducing senescence in neighboring cells. Modulating senescence or its associated secretory phenotype may offer a novel target for therapy in future trials.

Abbreviations: BrdU, 5-Bromo-2'-deoxyuridine; DAPI, 4',6-Diamidino-2-phenylindole; DMEM, Dulbecco's modified eagle's medium; FCS, Fetal calf serum; Gy, Gray; HCC, Hepatocellular carcinoma; HDR-BT, High-dose radiation brachytherapy; NPX, Normalized protein expression; PEA, Proximity extension assay; PBS, Phosphate-buffered saline; RIBE, Radiation-induced bystander effect; RPMI, Roswell park memorial institute medium; SASP, Senescence-associated secretory phenotype.

^a Department of Radiology, LMU University Hospital, LMU Munich, Marchioninistr. 15, 81377 Munich, Germany

^b Department of Radiation Oncology, LMU University Hospital, LMU Munich, Marchioninistr. 15, 81377 Munich, Germany

^c Department of Radiology, Hadassah Hebrew University Medical Center, 12000 Jerusalem, Israel

^{*} Corresponding author.

E-mail address: marianna.alunni@med.uni-muenchen.de (M. Alunni-Fabbroni).

¹ Present address: Department of Medicine II, LMU University Hospital, LMU Munich, Marchioninistr. 15, 81377, Munich, Germany.

² Contributed equally to this work.

Introduction

Local ablation allows for a minimally invasive cancer treatment enabling targeting the malignant tissue while sparing the adjacent, healthy tissues. It presents several advantages with respect to traditional surgery including being minimally invasive and preserving the organ functions. High-dose rate brachytherapy (HDR-BT) is a radiation-based method where radioactive sources are inserted directly inside or near the tumor, e.g., via the image-guided placement of catheters serving as guide-ropes for the radiation source. High doses of radiation can be delivered with optimal tumor targeting. HDR-BT offers excellent outcomes with lower radiation toxicity than conventional approaches and can overcome limitations of other local ablative, heat-based techniques such as microwave or radiofrequency ablation. This includes safely treating larger tumors and tumors adjacent to vessels due to heat-sink effects being avoided [1]. Furthermore, HDR-BT is often combined with external or systemic therapy is widely applied to different types of tumors including hepatocellular carcinoma (HCC) [2,3]. Despite the advantages offered by local hepatic ablation, tumor recurrence remains a major limitation and challenge in clinical practice. Tumors can exhibit therapy resistance, which can be linked to an insufficient cellular death, or to the activation of survival pathways that may promote or accelerate the known progressive cascade of tumorigenesis in the inflamed / cirrhotic liver [4-6]. Studies conducted in plasma from HCC patients treated with thermal ablation have shown increases of pro-tumorigenic proteins such as Interleukin-6, epidermal growth factor (EGF) and fibroblast growth factor 2 (FGF-2) which induce a strong cellular proliferation [7]. Similar results have also been found in HCC patients treated with HDR-BT [8], suggesting that local tumor ablation can be responsible for the release of relevant pro-tumorigenic mediators.

In recent years, the role of senescence in triggering therapy resistance in radiation-based therapy has become of ever-increasing interest. Radiation effectively induces cellular damage leading to apoptosis or senescence [9]. While apoptosis eliminates damaged cells in a controlled manner, senescent cells undergo permanent cell cycle arrest, becoming resistant to apoptosis while remaining metabolically active [10]. Moreover, senescent cells can acquire the so-called "senescence-associated secretory phenotype" (SASP), characterized by the secretion of diverse proteins including pro-inflammatory factors such as interleukins, cytokines, and growth factors [11]. Accumulating evidence points to the involvement of SASP-cells in the radiation-induced bystander effect (RIBE) on non-irradiated cells in which non-irradiated cells are affected by signals from nearby irradiated cells [12]. Moreover, it has been shown that SASP-cells ultimately induce chronic inflammation, contributing to tumorigenesis, metastasis formation, and therapy resistance [13-15]. In this study, we developed an in vitro HDR-BT system mimicking clinical radiotherapy protocols. Our aim was to demonstrate the effect of HDR-BT on senescence and the relationship between HDR-BT and the radiation-induced bystander effect in HCC cell lines.

Material and methods

Cell lines

HepG2 (p53-wild type), Huh7 (p53-mutant Y220C), and Hep3B (p53-null) cell lines were obtained from BLINDED. Short tandem repeats (STR) profiling of the cell lines was conducted by DSMZ – German Collection of Microorganisms and Cell Cultures GmbH (Braunschweig, Germany). A detailed description is given in Supplementary Data.

In vitro brachytherapy

Cell irradiation was performed in 6 or 96 well plates (Sarstedt, Nümbrecht, Germany). The outer dimension of the plates was 125×85 mm². The irradiation source was Iridium-192 from a Flexitron

afterloading device (Nucletron, Veenendaal, Netherlands) with an activity between 200 and 370 GBq (5–10 Ci). Cell were irradiated with 7.5 Gray (Gy), a dose which better approximates the sub-lethal conditions found in the tumor margins [16]. Irradiation ranged between 15 and 30 min, based upon on the source strength. Details are available in Supplementary data and Supplementary Fig. S1.

Conditioned medium

To generate conditioned medium (consisting of culture medium collected from irradiated cells and enriched with secreted proteins), cells were seeded in 6-well plates at a density of 350,000 cells/well, irradiated at a dose of 7.5 Gy and incubated at 37 °C with 5 % CO $_2$. Supernatants (i.e., conditioned medium) were collected at selected time points (30 min, 90 min, 24 h, 48 h, 72 h, 7 days) and immediately stored at $-80\,^{\circ}\mathrm{C}$ until further use. For comparison, the supernatant collected from non-irradiated cells (control medium), processed under identical conditions, was utilized as a control. For each time point, the resulting conditioned medium was collected and administered to a second batch of naïve, non-irradiated HepG2 cells to evaluate the effect on their growth. To accomplish this, naïve cells were continuously maintained in the presence of either conditioned medium or control medium (collected from non-irradiated cells at the same time points) for an additional 24 h, 48 h, or 72 h, without any refresh of the medium.

Bromodeoxyuridine (BrdU) assay

Cells were seeded into 8-well chambers (Sarstedt, Nümbrecht, Germany) at a density of 30,000 cells/well, and incubated in the presence of conditioned medium or control medium for 24 h, 48 h, or 72 h. BrdU (5-Bromo-2'-deoxyuridine) incorporation was measured using the colorimetric Cell Proliferation Kit according to manufacturer instructions (#11647229001, Sigma-Aldrich, St. Louis, MO, USA). The detailed protocol is described in Supplementary Data.

Cell number determination

The number of cells per plate was counted after exposure of the cells to the conditioned medium or the control medium at selected time points (24 h, 48 h and 72 h). Briefly, cells were detached using Accutase (PromoCell GmbH, Heidelberg, Germany) and diluted with PBS to a final volume of 1 mL. The cell suspension was centrifuged at 500 g, 4 $^{\circ}$ C for 5 min, supernatant aspirated, and the cell pellet reconstituted in 1 mL PBS. The number of cells was counted manually by a Neubauer hemocytometer under a light microscope..

Clonogenic assay

Cells were seeded into 6-well plates at a density of 1,000 cells/well and incubated for 14 days in the presence of conditioned medium or control medium. Both conditioned medium and control medium were substituted with a newly irradiated medium and fresh control medium after 7 days to avoid nutrient deprivation. Cells were then fixed in 3.7 % formaldehyde and stained with 0.5 % (w/v) crystal violet (Sigma-Aldrich) to visualize the colonies. The number of colonies with >50 cells were assessed for each condition.

Ki-67 quantification

Cells were seeded into 24-well plates at a density of 30,000 cells/well, and incubated in the presence of conditioned or control medium for 48 h, 72 h, 96 h, and 7 days. The detailed protocol is described in Supplementary Data.

Beta-galactosidase assay

Cells were seeded into 6-well plates at a density of 200,000 cell/well and incubated for 48 h, 72 h, 96 h, and 7 days in the presence of conditioned or control medium. The assay was performed using the Senescence Cells Histochemical Staining Kit according to manufacture instructions (# CD0030-1KZ, Sigma-Aldrich). Briefly, cells were washed with PBS, fixed and stained at 37 $^{\circ}$ C for 6 h. Stained and unstained cells were counted, and the percentage of positive cells was calculated.

Proximity Extension Assay

Proteins were measured in 1 μ L of conditioned medium using the Olink proteomics Target 96 Immuno-Oncology and Inflammation panels (Olink Proteomics, Uppsala, Sweden) based on Proximity Extension Assay (PEA) technology [17,18] The detailed protocol is described in Supplementary Data and Supplementary File 1 for the full list of proteins.

Statistical analysis

Significant differences among the different experimental groups were tested using an unpaired Mann-Whitney test in Prism 5 (GraphPad Prism, Version 10.2.3, 2024). Protein–protein interaction (PPI) networks were analyzed using the STRING database (https://string-db.org/).

Results

To test the influence of radiation on cellular proliferation, HepG2 cells were irradiated and incubated for 30 min, 90 min, 24 h, or 48 h. At each time point, medium was collected and applied to naïve, non-irradiated HepG2 cells, which were then incubated for additional 24 h, 48 h, or 72 h and screened for DNA synthesis. The highest rate of BrdU incorporation was observed in naïve cells exposed to conditioned medium collected 90 min post-irradiation, with ratios of 0.264 (standard deviation, SD:0.01) after 24 h and 0.246 (SD:0.08) after 48 h of exposure, consistent with previous findings [7] (Fig. 1A). A marked reduction

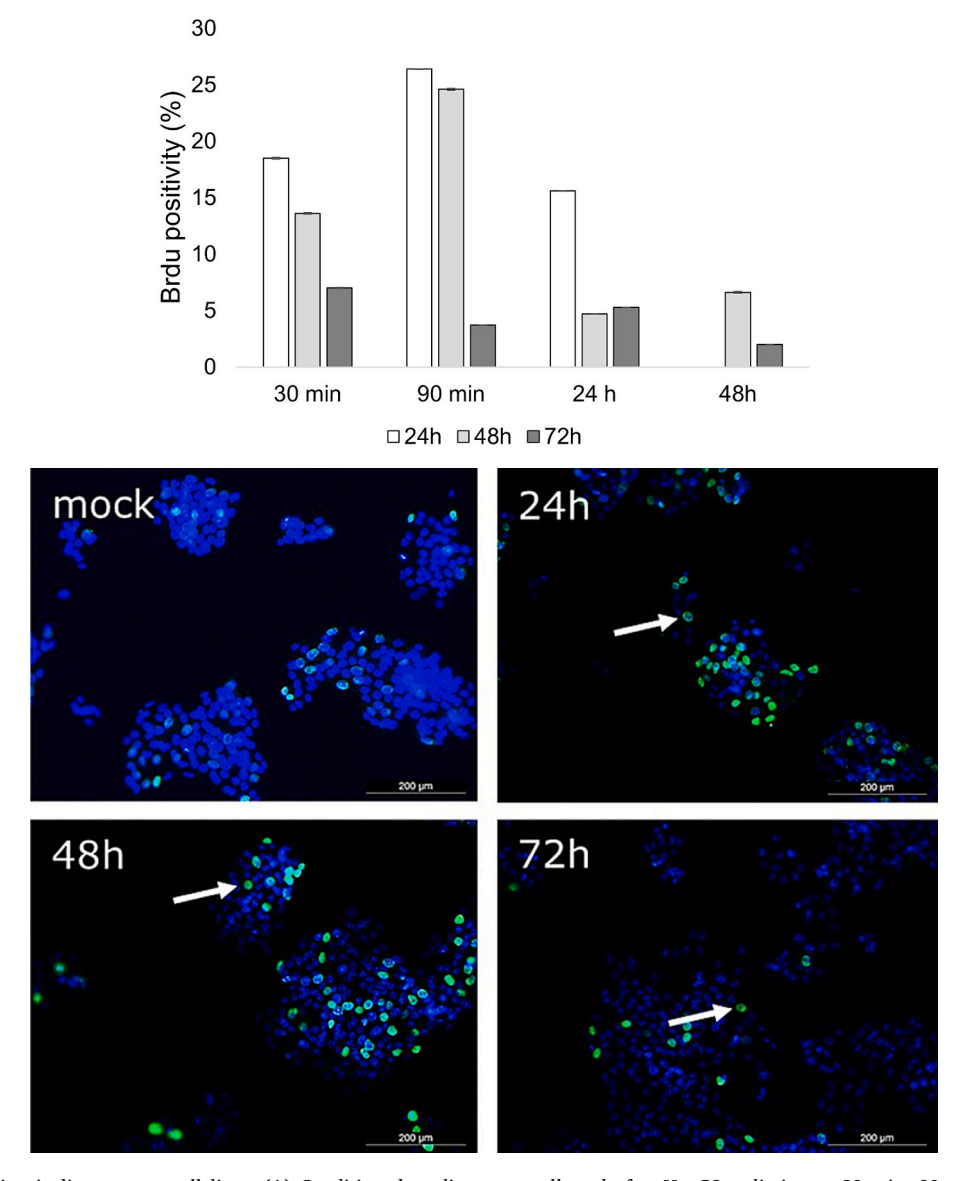


Fig. 1. BrdU incorporation in liver cancer cell lines. (A) Conditioned medium was collected after HepG2 radiation at 30 min, 90 min, 24 h, and 48 h, and administered to naïve HepG2. HepG2 were then left in the presence of conditioned medium for additional 24 h, 48 h, and 72 h. (B) Representative images of HepG2 incubated for 24 h, 48 h, and 72 h with conditioned medium collected 90 min post radiation. The arrows indicate BrdU positive cells. Nuclei are stained with DAPI (x20, scale bar 200 μm).

in BrdU positive cells was observed at 72 h (Fig. 1B). Based on these observations, the 90 min time point was chosen for subsequent medium collection. To validate this observation, viable cell counts were quantified using a Neubauer hemocytometer. The total number of HepG2 cells remained stable during the first 48 h, but decreased by 20 % at 72 h. For similar experimental conditions conducted on two additional HCC cell lines, Huh7 cells revealed a comparable trend, whereas Hep3B showed an increase in cell number (Fig. 2). Since HepG2 and Huh7 differ from Hep3B in the expression of the tumor suppressor gene p53 (wild type in HepG2, constitutively active in Huh7, null in Hep3B), we hypothesized that the effect of the conditioned medium on naïve cells might be modulated by this protein. To investigate this, we tested the effect of the conditioned medium collected from HepG2 cells on naïve Hep3B cells. In concordance with prior research, we found that p53-null Hep3B cells did not exhibit a measurable response to the conditioned medium derived from HepG2 cells. This lack of response suggests that the factors secreted by HepG2 cells require functional p53 signaling to exert their effects, a pathway that is absent in Hep3B cells due to their p53-null status. By contrast, applying conditioned medium from Hep3B cells to HepG2 cells yielded different results as Hep3B-conditioned medium failed to produce this effect in HepG2 cells (despite the fact that HepG2conditioned medium triggers a peak in BrdU incorporation within the first 48 h). This suggests that the factors secreted by Hep3B cells are not capable of inducing the same proliferative response in HepG2 cells as the HepG2-conditioned medium does in itself indicating an autocrine mechanism. The absence of a similar response with Hep3B-conditioned medium further supports the idea that this effect is specific to HepG2 cells and is not merely due to general soluble factors present in conditioned media (data not shown).

To clarify the influence of conditioned medium on growth dynamics, the expression level of Ki-67 was determined in both HepG2 and Hep3B cell lines. In HepG2 cells, the proportion of Ki-67-positive cells significantly decreased from 80 % to 20 % following treatment with conditioned medium. By contrast, Hep3B cells showed an increase in Ki-67 expression reaching more than 90 % positivity after 96 h of incubation (Fig. 3). To further investigate the impact of conditioned medium on cellular proliferation, we conducted colony formation assays with both HepG2 and Hep3B cell lines. Consistent with the Ki-67 results, HepG2 cells demonstrate marked reduced clonogenicity capacity following exposure to conditioned media, with an average of 631 colonies

compared to 1,707 colonies observed in control medium conditions, corresponding to a decrease of 63 %. By contrast, Hep3B cells exhibited an increased, near doubling in clonogenic potential response to conditioned medium, with an average of 436 colonies compared to 260 colonies in the control group, with an increase of 67 % (Fig. 4). The concordant findings from Ki-67 expression analysis and colony formation assays strongly indicate that conditioned medium suppresses proliferation in HepG2 (p53 $^+$ /p21 $^+$) cells, but not in Hep3B (p53 $^-$ /p21 $^-$) cells, highlighting the critical role of the p53 pathway in mediating this selective inhibitory response.

Next, to explore the composition of HepG2's conditioned medium, we conducted a secretome analysis comprised of 192 proteins. This proteomic profiling revealed enrichment of 29 proteins with a robust increase in abundance (log2 fold change greater than 1.5) compared to the control medium (Table 1). Notably, of these 29 proteins, 15 (51.5 %) were identified as a component of the SASP.

Given that conditioned medium was enriched with senescence-inducing factors and considering that radiation is known to trigger cell cycle arrest through the activation of senescence, we evaluated the induction of senescence in HepG2 and Hep3B cells exposed to conditioned medium at different time points using beta-galactosidase staining. In HepG2 cells, an increase of beta-galactosidase positivity was observed after 72 h of incubation with the conditioned medium, while cells incubated with control medium exhibited only minimal positivity at similar time points, becoming noticeable only after 7 days (Fig. 5). By contrast, Hep3B cells did not show significant differences in senescence between those exposed to the conditioned medium and the negative control (data not shown). Notably, in donor cells, the first signs of senescence, manifest by increased beta-galactosidase activity, were observed at 48 h post-radiation, despite the early presence of SASP-associated proteins in the conditioned medium (data not shown).

Finally, we compared the secretome composition of supernatants collected from naïve cells after various incubation times with the conditioned medium. Since the half-life of secreted cytokines and growth factors is typically short ranging from a few minutes to a few hours — we hypothesized that the secretome composition observed in the supernatant of cells incubated with the conditioned medium for over 48 h primarily reflected molecules secreted by the cells themselves, rather than the original constituents of the conditioned medium. Proteomic profiling of the supernatants revealed an enrichment of proteins,

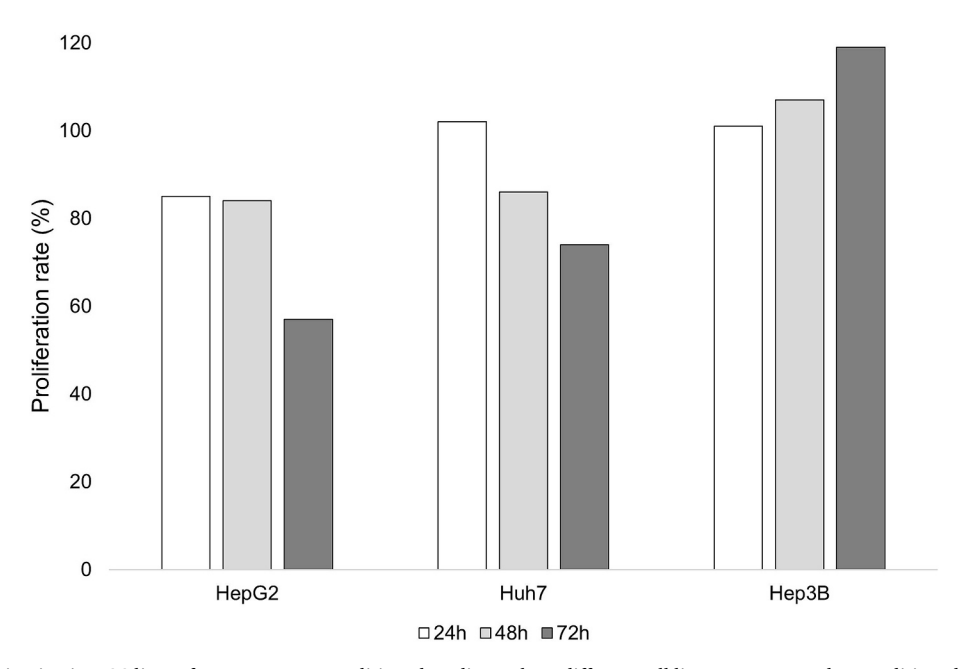
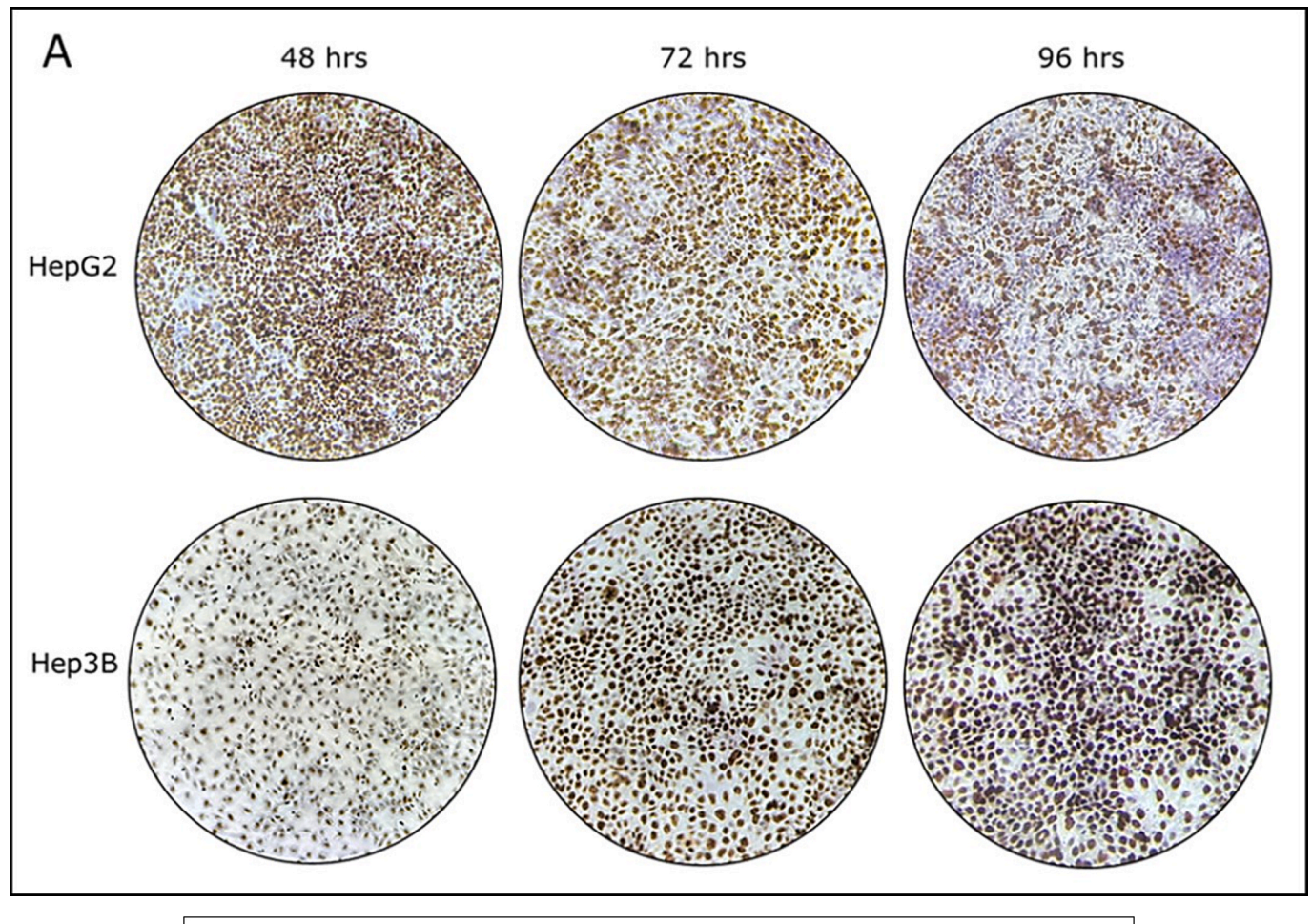


Fig. 2. Cell count determination in HCC lines after exposure to conditioned medium. Three different cell lines were exposed to conditioned medium collected 90 min post radiation for 24 h, 48 h, or 72 h and manually counted using a Neubauer hemocytometer under a light microscope.



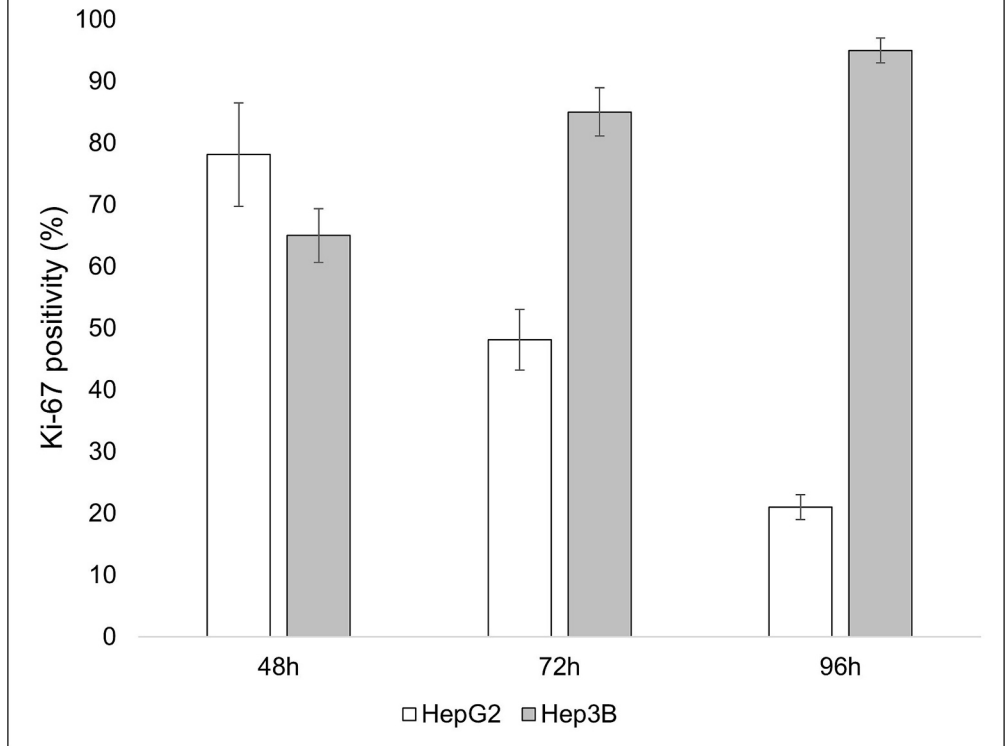


Fig. 3. Ki-67 expression by IHC in HepG2 and Hep3B. (A) Representative images of Ki-67 staining in HepG2 and Hep3B following 48 h, 72 h, or 96 h exposure to conditioned medium collected 90 min post radiation. (B) Ki-67 positivity expressed as % of positive cells.

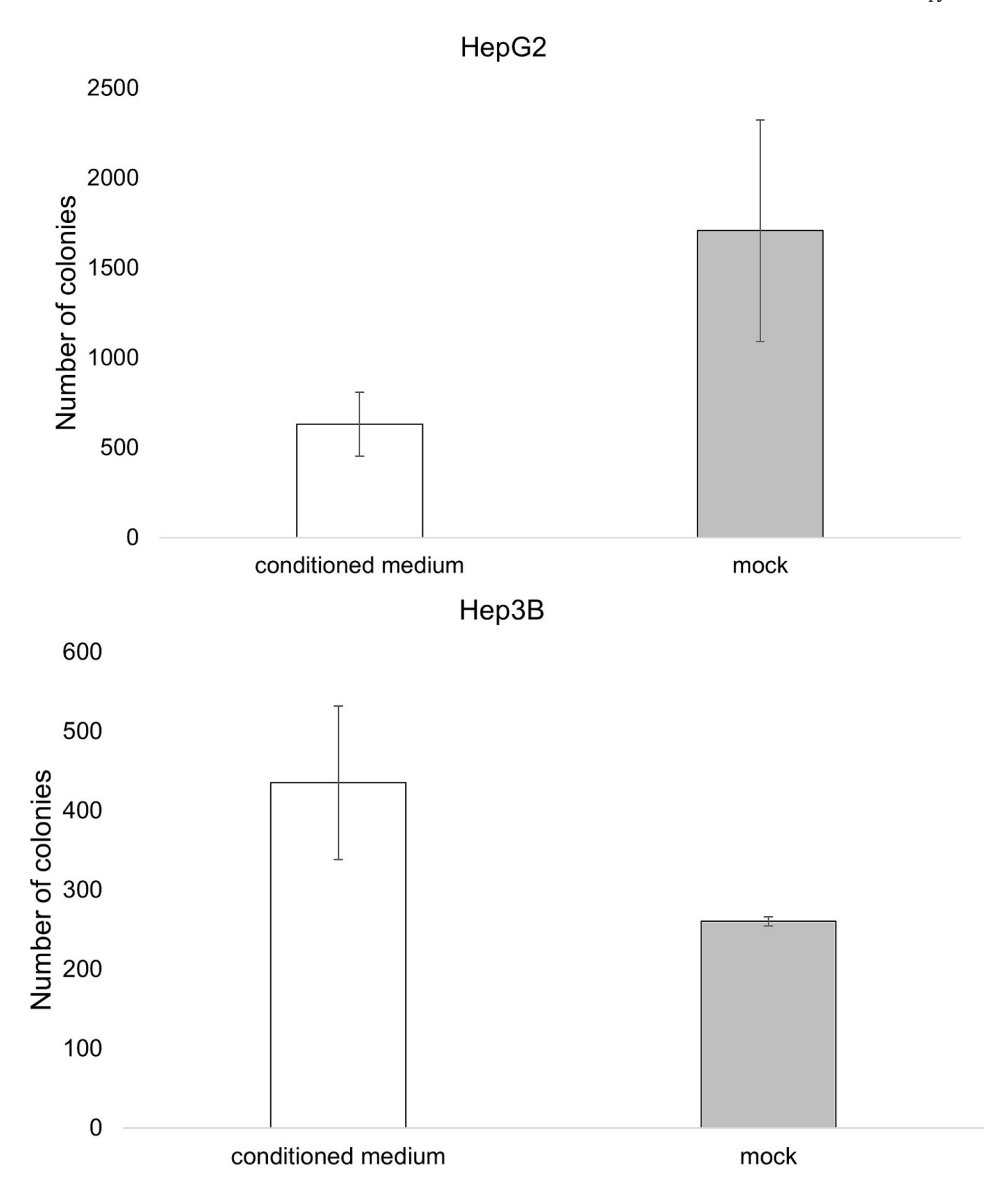


Fig. 4. Clonogenic survival assay. HepG2 and Hep3B cells were seeded in 6-well plates and incubated with conditioned medium collected 90 min after radiation. Following a 2-week incubation period, the number of colonies was counted.

with 18 proteins showing an increased fold change greater than 1.5 at 48 h, 34 proteins at 72 h and 19 proteins at 96 h (for the complete list, Sup. Table S2). At 72 h we observed an overlapping profile that included 9 SASP proteins shared between the conditioned medium and the supernatant (Fig. 6A). To explore the role of the proteins found in both the supernatants collected from the donor and naïve cells, we performed a STRING-based protein–protein interaction (PPI) analysis (Fig. 6B). Six out of 9 proteins displayed a strong connection with IL1-alpha, a known regulator of senescence via the activation of SASP. In order to better understand this finding, we extended the proteomic analysis to include medium collected 30 min after radiation. Here, we found only three proteins, which were overexpressed with a fold change > 1.5 including IL1alpha (MMP7, fold change: 3.781; IL1 alpha, fold change: 2.417; and CAIX, fold change 1.543).

Discussion

Radiation therapy is highly effective in targeting and destroying tumors. However, it also can induce RIBE on non-targeted tissues [19,20]. These effects are mediated by the release of molecules such as

cytokines and growth factors, which can trigger chronic inflammation and potentially promote tumor recurrence [21]. In this study, we present an in vitro brachytherapy model demonstrating a rapid increase in DNAsynthesis in HCC cell lines, which abates within 72 h post-radiation and is not followed by anticipated cellular division. Furthermore, applying the supernatant from irradiated cells to naïve, non-irradiated cells recapitulates the same effects, indicating that the conditioned medium alone can mimic the radiation RIBE effect. The rationale for selecting a 7.5 Gy dose stems from evidence that, in clinical settings, a standard 15 Gy dose effectively ablates the tumor core but delivers significantly lower doses to the margins [16]. These peripheral regions often harbor metabolically active, radioresistant cells and are common sites of recurrence [22]. Accordingly, targeting this sub-lethal dose range allows focused investigation of marginal zone responses where pro-tumorigenic phenotypes may emerge. Molecular analysis shows that the naïve cells after incubation with the irradiated supernatant do not divide robustly as anticipated, as shown by a drastic reduction in Ki-67 expression, while concomitantly showing an increase in senescence. Moreover, proteomic profiling of the conditioned medium reveals an enrichment of SASP-associated proteins. Remarkably, the naïve cells after exposure to

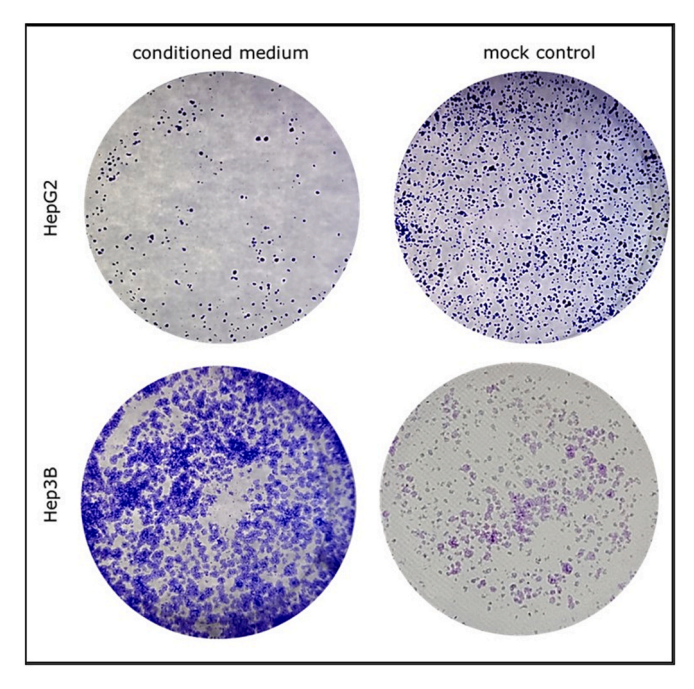


Fig. 4. (continued).

Table 1Secretome analysis of conditioned medium collected 90 min post radiation. SASP proteins are indicated with an asterisk.

Inflammation		Immuno-oncology	
	Fold change		Fold change
IL-24	3.575	MMP-7*	3.761
CCL4*	2.523	HO-1	2.449
Flt3L	2.390	CD40*	1.956
MCP-3*	2.307	IFN-gamma*	1.880
IL-22 RA1	2.236	CAIX	1.796
FGF-23*	2.167	CASP-8	1.725
SIRT2*	2.102	NCR1	1.572
CD6	1.936	CX3CL1	1.553
CCL25*	1.934	PTN	1.552
FGF-5*	1.931		
NT-3	1.855		
TNFSF14*	1.837		
CXCL5*	1.802		
IL8*	1.755		
SLAMF1	1.735		
CCL11*	1.708		
ARTN	1.702		
MMP-10*	1.642		
CXCL1*	1.606		
IL5	1.510		

the conditioned medium produce their own SASP-enriched secretome, showing an overlap with conditioned medium of 60 %. This finding suggests an autocrine loop that potentially perpetuates senescence and therefore the production of SASP-associated proteins. We must acknowledge that the proteomic data obtained from naïve cells exposed to conditioned medium must be interpreted with caution, as distinguishing newly secreted proteins from those carried over from the original medium remains challenging. However, given that secreted proteins generally have relatively short half-lives, typically ranging from hours to a few days due to extracellular degradation [23–26], it is most likely that many of the proteins detected after incubation are likely to be newly secreted.

Senescence is a physiological process typically triggered by telomere shortening, which halts the cell cycle to safeguard against genomic instability. However, stress-related factors such as increased reactive oxygen species (ROS), DNA damage, and epigenetic changes can also induce senescence [27]. Therapies such as radiation and chemotherapy promote cellular senescence by causing DNA breaks that activate DNA damage response (DDR). This, in turn, triggers cell cycle arrest via activation of the tumor suppressor p53. If DNA repair fails and growth arrest persists, p53 induces senescence through cyclin-dependent kinase inhibitors such as p21 and p16. Our study compared the responses of p53-wild type HepG2 with p53-null Hep3B cells. Conditioned medium caused reduced cell proliferation and increased senescence in HepG2, but not in Hep3B cells, supporting the hypothesis that conditioned medium exerts effects through pathways resembling those activated by direct radiation exposure via p53. In line with our findings in HCC cell lines, it was previously demonstrated that co-incubating irradiated colorectal cancer cells with naïve cells strongly induces senescence in p53-positive cell populations, highlighting the role of p53 as a key regulator of senescence [28,29]. In conclusion, our work demonstrates, in in vitro HCC cell lines, that conditioned medium from irradiated cells recapitulates many of the biological effects observed following direct radiation exposure. This suggests that radiation-induced secreted factors alone are sufficient to trigger key cellular responses in non-irradiated liver cancer cells, highlighting the importance of the tumor microenvironment and bystander signaling in radiotherapy outcomes.

A hallmark of cellular senescence is the secretion of proinflammatory cytokines, growth factors, and proteases secreted by cells that show SASP [30]. These SASP-associated proteins serve a dual role: they reinforce the senescent state via autocrine signaling while promoting proliferation in neighboring non-senescent cells. In our study, conditioned medium collected 90 min after radiation exposure exhibited elevated concentrations of 15 SASP-associated proteins, with CCL4 and MCP3 showing the highest levels. Notably, no evidence of senescence was observed in donor cells at this early time point. The first signs of senescence emerged 48 h post-radiation. These findings suggest that radiation triggers the release of SASP-associated proteins independently of senescence onset in donor cells, and that SASP-associated proteins drive senescence in neighboring non-targeted cells through a bystander effect, maintaining their secretion in the microenvironment. These findings have significant implications for understanding how tumor treatments influence naïve cells, altering their growth patterns and secretome. Radiation therapy halts cell growth and enhances

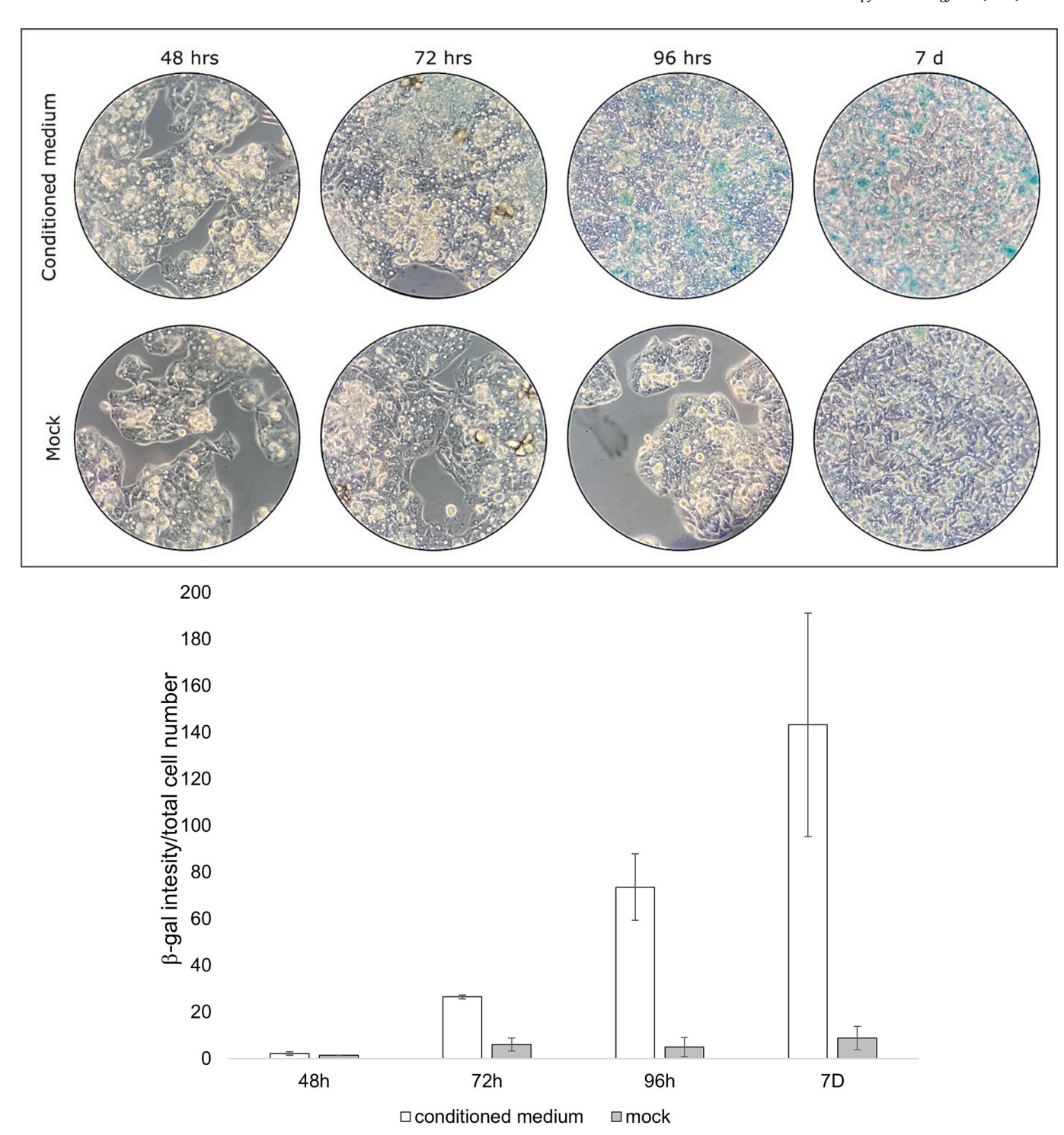
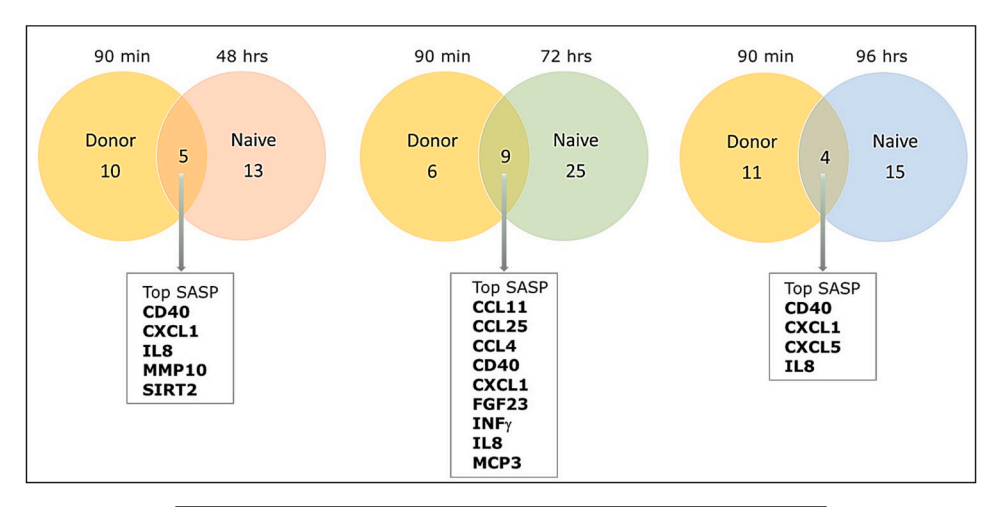


Fig. 5. Senescence associated (SA)-beta-galactosidase staining. HepG2 cells were seeded in 6-well plates and incubated with conditioned medium or control medium for 48 h, 72 h, 96 h and 7 days. After each time point, cells were fixed stained for beta-galactosidase activity. (A) Representative images of SA-beta-galactosidase staining. (B) Quantification of SA-beta-galactosidase activity.

immune surveillance for subsequent clearance of senescent cells [31]. Yet, if senescent cells are not efficiently cleared, their metabolic activity can foster tumor recurrence [32].

To address this challenge, so-called senolytic therapies aiming to selectively eliminate senescent cells following primary treatment are being explored [33,34]. The "One-Two Punch"-approach whereby at first the patient is treated with a therapy targeting the tumor cells, then the patient receives a senolytic therapy targeting the senescence cells [35,36] has shown effectiveness in cancer treatment in pre-clinical

trials. Another approach to control the adverse effect of senescence on cancer therapy is the use of senomorphic SASP-inhibitors. Among others, rapamycin, an inhibitor of mTOR has shown capability to suppress pro-inflammatory and pro-tumorigenic SASP *in vitro* and in animal models [37]. Furthermore, antibodies against IL-6 (associated with senescence mechanisms) have been tested in pre-clinical trials on different cancer types [38,39]. We must acknowledge several limitations of this work. Only one radiation dose was used and radiation was administered only to HCC cell lines. In the clinical setting, a wide variety



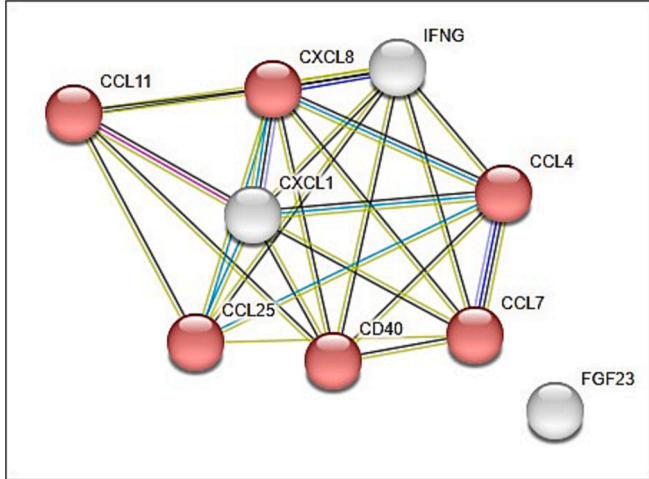


Fig. 6. Comparison between the protein profiles in medium collected from irradiated and naïve cells at different time points. (A) Venn diagrams were used to compare the top proteins (fold change relative to control medium ≥ 1.5) identified in the conditioned medium collected 90 min post-radiation with those in the supernatants collected from naïve cells after incubation with the conditioned medium for 48 h, 72 h, and 96 h. (B) STRING analysis (http://string-db.org) uncovering protein–protein interactions of upregulated proteins identified in the secretome of donor and naïve cells. Each node (n = 9) represents a protein, and each edge (n = 25) represents an interaction including either physical or functional associations. PPI enrichment p = 9.1e-15.

of tumor types and native cell populations, including not only hepatocytes, but also endothelial cells, cholangiocytes, and stellate cells can experience bystander effect due to radiation. Future experiments expanding the cell lines and the radiation dosages will be necessary to validate our findings. Furthermore, the *in vitro* radiation model we have used in this work was performed on a 2D cellular model which does not entirely reflects the physiological conditions of a tumor. We recognize the critical importance of further validating our *in vitro* findings using in vivo animal models, as this step is essential for enhancing the translational relevance of our research and ensuring that our results can be meaningfully applied in physiological and clinical contexts. Given that our *in vitro* model does not fully capture the complexity of the tumor microenvironment, further studies in more physiologically relevant systems are warranted.

In conclusion, this study demonstrates that HDR-BT induces a bystander effect in HCC cell lines, most likely mediated by SASP-associated proteins that drive senescence in non-targeted cells through a p53-dependent mechanism. SASP secretion occurs independently of senescence onset in donor cells, highlighting a complex radiation response. While radiation therapy is effective in suppressing tumor growth, persistent senescent cells within the tumor microenvironment may contribute to recurrence and therapy resistance. Therefore, targeting senescence with senolytics or SASP inhibitors into treatment regimens holds promise for enhancing long-term therapeutic efficacy

and preventing cancer relapse.

Data Availability Statement

All data being analyzed as part of this study are included in this manuscript and the supplementary materials. Further inquiries can be sent to the corresponding author.

Funding source

This research did not receive any specific grant from funding agencies in the public, commercial, or not-for-profit sectors.

CRediT authorship contribution statement

Josephine Naruhn: Writing – review & editing, Writing – original draft, Visualization, Validation, Project administration, Methodology, Investigation, Formal analysis, Data curation, Conceptualization. Moritz N. Gröper: Writing – review & editing, Writing – original draft, Visualization, Validation, Project administration, Methodology, Investigation, Formal analysis, Data curation, Conceptualization. Elif Öcal: Writing – review & editing, Investigation. Lukas Salvermoser: Writing – review & editing, Formal analysis. Heidrun Hirner-Eppeneder: Writing – review & editing, Investigation. Jan N. Schäfer: Writing – review & editing, Formal analysis. Philipp M. Kazmierczak: Writing – review & editing, Methodology. Stephanie Corradini: Writing – review & editing, Resources, Methodology. Justus-Christian Well: Resources, Investigation. Jens Ricke: Writing – review & editing, Supervision,

Resources, Conceptualization. **S. Nahum Goldberg:** Writing – review & editing, Writing – original draft, Supervision, Conceptualization. **Matthias Stechele:** Writing – review & editing, Supervision, Resources, Project administration, Methodology, Formal analysis, Conceptualization. **Marianna Alunni-Fabbroni:** Writing – review & editing, Writing – original draft, Visualization, Validation, Supervision, Resources, Project administration, Methodology, Investigation, Formal analysis, Data curation, Conceptualization.

Declaration of competing interest

SNG: Consultant to Snipe Medical Technology, Rehovot Israel and supported by Israel Science Foundation research grant (ISF 2026/2024). All remaining authors have declared no competing interest.

Appendix A. Supplementary data

Supplementary data to this article can be found online at https://doi.org/10.1016/j.radonc.2025.111068.

References

- Liu Z, Ahmed M, Sabir A, Humphries S, Goldberg SN. Computer modeling of the effect of perfusion on heating patterns in radiofrequency tumor ablation. Int J Hyperth 2007; 23:49–58.
- [2] Rizzo A, Ricci AD, Brandi G. Systemic adjuvant treatment in hepatocellular carcinoma: tempted to do something rather than nothing. Future Oncol 2020;16:2587–9.
- [3] Vogel A, Cervantes A, Chau I, Daniele B, Llovet JM, Meyer T, et al. Hepatocellular carcinoma: ESMO Clinical Practice guidelines for diagnosis, treatment and follow-up. Ann Oncol 2018;29.
- [4] Hanggi K, Ruffell B. Cell death, therapeutics, and the immune response in cancer. Trends Cancer 2023;9:381–96.
- [5] Neophytou, C.M., I.P. Trougakos, N. Erin, and P. Papageorgis, Apoptosis Deregulation and the Development of Cancer Multi-Drug Resistance. Cancers (Basel), 2021. 13(17).
- [6] Hanahan D. Hallmarks of Cancer: New Dimensions. Cancer Discov 2022;12:31-46.
- [7] Markezana A, Paldor M, Liao H, Ahmed M, Zorde-Khvalevsky E, Rozenblum N, et al. Fibroblast growth factors induce hepatic tumorigenesis post radiofrequency ablation. Sci Rep 2023;13:16341.
- [8] Salvermoser L, Goldberg SN, Alunni-Fabbroni M, Kazmierczak PM, Groper MN, Schafer JN, et al. CT-guided high dose rate brachytherapy can induce multiple systemic proteins of proliferation and angiogenesis predicting outcome in HCC. Transl Oncol 2024;43:101919.
- [9] Eriksson D, Stigbrand T. Radiation-induced cell death mechanisms. Tumour Biol 2010;31:363–72.
- [10] Gorgoulis V, Adams PD, Alimonti A, Bennett DC, Bischof O, Bishop C, et al. Cellular Senescence: defining a Path Forward. Cell 2019;179:813–27.
- [11] Coppe JP, Desprez PY, Krtolica A, Campisi J. The senescence-associated secretory phenotype: the dark side of tumor suppression. Annu Rev Pathol 2010;5:99–118.
- [12] Tang H, Cai L, He X, Niu Z, Huang H, Hu W, et al. Radiation-induced bystander effect and its clinical implications. Front Oncol 2023;13:1124412.
- [13] Takasugi M, Yoshida Y, Hara E, Ohtani N. The role of cellular senescence and SASP in tumour microenvironment. FEBS J 2023;290:1348–61.
- [14] Dong Z, Luo Y, Yuan Z, Tian Y, Jin T, Xu F. Cellular senescence and SASP in tumor progression and therapeutic opportunities. Mol Cancer 2024;23:181.
- [15] Faggioli F, Velarde MC, Wiley CD. Cellular Senescence, a Novel Area of Investigation for Metastatic Diseases. Cells 2023;12.

- [16] Seidensticker M, Wust P, Ruhl R, Mohnike K, Pech M, Wieners G, et al. Safety margin in irradiation of colorectal liver metastases: assessment of the control dose of micrometastases. Radiat Oncol 2010;5:24.
- [17] Assarsson E, Lundberg M, Holmquist G, Bjorkesten J, Thorsen SB, Ekman D, et al. Homogenous 96-plex PEA immunoassay exhibiting high sensitivity, specificity, and excellent scalability. PLoS One 2014;9:e95192.
- [18] Petrera A, von Toerne C, Behler J, Huth C, Thorand B, Hilgendorff A, et al. Multiplatform Approach for Plasma Proteomics: Complementarity of Olink Proximity Extension Assay Technology to Mass Spectrometry-based Protein Profiling. J Proteome Res 2021;20:751–62.
- [19] Kim J, Jung Y. Radiation-induced liver disease: current understanding and future perspectives. Exp Mol Med 2017;49:e359.
- [20] Zhu W, Zhang X, Yu M, Lin B, Yu C. Radiation-induced liver injury and hepatocyte senescence. Cell Death Discov 2021;7:244.
- [21] Chambers CR, Ritchie S, Pereira BA, Timpson P. Overcoming the senescenceassociated secretory phenotype (SASP): a complex mechanism of resistance in the treatment of cancer. Mol Oncol 2021;15:3242–55.
- [22] Barker HE, Paget JT, Khan AA, Harrington KJ. The tumour microenvironment after radiotherapy: mechanisms of resistance and recurrence. Nat Rev Cancer 2015;15: 409–25
- [23] Liu C, Chu D, Kalantar-Zadeh K, George J, Young HA, Liu G. Cytokines: from Clinical significance to Quantification. Adv Sci (Weinh) 2021;8:e2004433.
- [24] Miyakawa N, Nishikawa M, Takahashi Y, Ando M, Misaka M, Watanabe Y, et al. Prolonged circulation half-life of interferon gamma activity by gene delivery of interferon gamma-serum albumin fusion protein in mice. J Pharm Sci 2011;100:2350–7.
- [25] Berchiche YA, Gravel S, Pelletier ME, St-Onge G, Heveker N. Different effects of the different natural CC chemokine receptor 2b ligands on beta-arrestin recruitment, Galphai signaling, and receptor internalization. Mol Pharmacol 2011;79:488–98.
- [26] Chen W, Smeekens JM, Wu R. Systematic study of the dynamics and half-lives of newly synthesized proteins in human cells. Chem Sci 2016;7:1393–400.
- [27] Hayes JD, Dinkova-Kostova AT, Tew KD. Oxidative stress in Cancer. Cancer Cell 2020;38:167–97.
- [28] Poleszczuk J, Krzywon A, Forys U, Widel M. Connecting radiation-induced bystander effects and senescence to improve radiation response prediction. Radiat Res 2015;183: 571–7.
- [29] Rodier F, Campisi J. Four faces of cellular senescence. J Cell Biol 2011;192:547-56.
- [30] Schoetz U, Klein D, Hess J, Shnayien S, Spoerl S, Orth M, et al. Early senescence and production of senescence-associated cytokines are major determinants of radioresistance in head-and-neck squamous cell carcinoma. Cell Death Dis 2021;12:1162.
- [31] Kang TW, Yevsa T, Woller N, Hoenicke L, Wuestefeld T, Dauch D, et al. Senescence surveillance of pre-malignant hepatocytes limits liver cancer development. Nature 2011; 479:547–51.
- [32] Eggert T, Wolter K, Ji J, Ma C, Yevsa T, Klotz S, et al. Distinct Functions of Senescence-Associated Immune responses in Liver Tumor Surveillance and Tumor Progression. Cancer Cell 2016;30:533–47.
- [33] Kim JH, Brown SL, Gordon MN. Radiation-induced senescence: therapeutic opportunities. Radiat Oncol 2023;18:10.
- [34] Imawari Y, Nakanishi M. Senescence and senolysis in cancer: the latest findings. Cancer Sci 2024:115:2107–16.
- [35] Ohtani N. The roles and mechanisms of senescence-associated secretory phenotype (SASP): can it be controlled by senolysis? Inflamm Regen 2022;42:11.
- [36] Galiana I, Lozano-Torres B, Sancho M, Alfonso M, Bernardos A, Bisbal V, et al. Preclinical antitumor efficacy of senescence-inducing chemotherapy combined with a nanoSenolytic. J Control Release 2020;323:624–34.
- [37] Wang R, Sunchu B, Perez VI. Rapamycin and the inhibition of the secretory phenotype. Exp Gerontol 2017;94:89–92.
- [38] Ortiz-Montero P, Londono-Vallejo A, Vernot JP. Senescence-associated IL-6 and IL-8 cytokines induce a self- and cross-reinforced senescence/inflammatory milieu strengthening tumorigenic capabilities in the MCF-7 breast cancer cell line. Cell Commun Signal 2017;15:17.
- [39] Jia D, Zhang F, Li H, Shen Y, Jin Z, Shi FD, et al. Responsiveness to Tocilizumab in Anti-Acetylcholine Receptor-positive Generalized Myasthenia Gravis. Aging Dis 2024; 15:824–30.